Molecular Crystals and Liquid Crystals Science and Technology. Section A. Molecular Crystals and Liquid Crystals
Publication details, including instructions for authors and subscription information:
http://www.tandfonline.com/loi/gmcl19

Fourier Transform Infrared Spectroscopic Conformational Analysis of a Liquid Crystal in Elevated Temperature Mesophases

C. S. Digiacomo [a], J. L. Koenig [a] & M. E. Neubert [b]
[a] Department of Macromolecular Science, Case Western Reserve University, Cleveland, OH, 44106
[b] Liquid Crystal Institute, Kent State University, Kent, OH, 44242
Version of record first published: 04 Oct 2006.

To cite this article: C. S. Digiacomo , J. L. Koenig & M. E. Neubert (1996): Fourier Transform Infrared Spectroscopic Conformational Analysis of a Liquid Crystal in Elevated Temperature Mesophases, Molecular Crystals and Liquid Crystals Science and Technology. Section A. Molecular Crystals and Liquid Crystals, 289:1, 149-167

To link to this article: http://dx.doi.org/10.1080/10587259608042319

Mol. Cryst. Liq. Cryst., 1996, Vol. 289, pp. 149–167
Reprints available directly from the publisher
Photocopying permitted by license only

Fourier Transform Infrared Spectroscopic Conformational Analysis of a Liquid Crystal in Elevated Temperature Mesophases

C. S. DIGIACOMO[a], J. L. KOENIG[a] and M. E. NEUBERT[b]

[a]*Department of Macromolecular Science, Case Western Reserve University, Cleveland, OH, 44106;*
[b]*Liquid Crystal Institute, Kent State University, Kent, OH, 44242*

(Received 26 April 1995; In final form 21 June 1996)

Conformations of the aromatic ether bonds located on the tetra-substituted benzene ring in 4-[3′,4′,5′,-Tri(*p*-*n*-dodecyloxybenzoyloxy) benzoyloxy]4″-*p*-*n*-dodecyloxybenzoyloxy-biphenyl were measured throughout the temperature ranges of the nematic and smectic C mesophases using Fourier transform infrared spectroscopy. An abrupt decrease in the angle between the bonds occurred at the transition from the nematic to the smectic C mesophase. The molecule adopted a more compact conformation to pack into the more highly ordered smectic C mesophase.

Keywords: Conformational; conformations; FT-IR; phase transitions

INTRODUCTION

Attainment of nematic-type liquid crystalline mesophases requires molecules which have an elongated structure [1, 2]; i.e., the molecules must have a rather large aspect ratio. Accordingly, the conformation of branched molecules will affect the molecule's aspect ratio and subsequent ability to attain liquid crystalline mesophases. Elucidation of molecular conformations of branched molecules in liquid crystalline mesophases can provide insight into why certain liquid crystalline mesophases are obtained and what, if any, transitions between these mesophases are precipitated by

changes in molecular conformation. To this end, the conformations of the aromatic ether bonds located on the tetra-substituted benzene ring in 4-[3′,4′,5′-Tri(*p*-*n*-dodecyloxybenzoyloxy) benzoyloxy] 4″-*p*-*n*- dodecyloxybenzoyloxy-biphenyl (Fig. 1) in the nematic and smectic C mesophases were studied using Fourier transform infrared spectroscopy.

BACKGROUND

To understand how molecular conformational analysis can be performed using Fourier transform infrared spectroscopy, consider first a set of three coplanar transition moment vectors separated by an angle θ as shown in Figure 2. Using the relationship between transition moment vectors and infrared absorbance [3], an expression for the dichroic ratio, R, of this situation can be easily derived and is shown in Figure 2. Imagine now a large number of randomly oriented molecules, each molecule featuring this group of three coplanar transition moment vectors separated by an angle θ

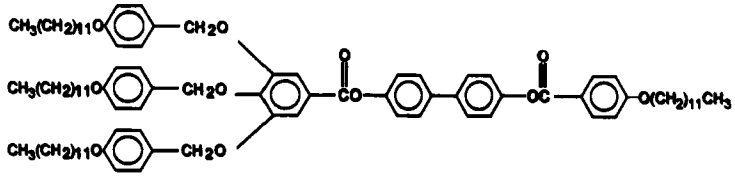

FIGURE 1 4-[3′,4′,5′-Tri(*p*-*n*-dodecyloxybenzoyloxy) benzoyloxy]4″-*p*-*n*-dodecyloxybenzoyloxy-biphenyl.

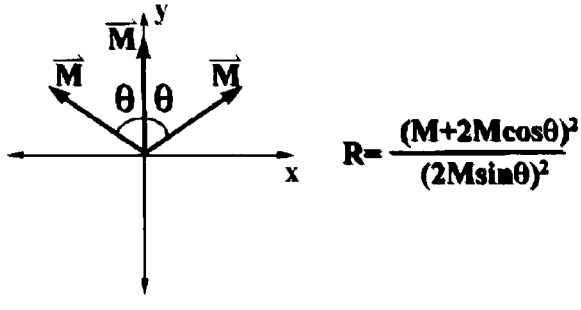

FIGURE 2 Three coplanar transition moment vectors separated by an angle θ and the expression for the dichroic ration, R, of this situation.

as shown in Figure 3a. Because the molecules are randomly oriented, the dichroic ratio of the infrared absorbance peak arising from these transition moment vectors will equal 1, regardless of the angle θ between the transition moment vectors. However, if some amount of uniaxial orientation is applied to the molecules, as shown in Figure 3b, then the dichroic ratio of the infrared absorbance peak arising from the transition moment vectors will no longer equal 1. The value that the dichroic ratio now equals will depend on two factors: the overall extent of orientation of the molecules and the angle θ between the transition moment vectors. Thus it is clear that Fourier transform infrared spectroscopy can be used for molecular conformational analysis.

This principle can be applied to the molecule being studied. The two adjacent para-substituted benzene rings, shown in red in Figure 4a, provide the rigid backbone type of structure necessary to procure nematic-type liquid crystalline mesophases. The stretching vibrations of the aromatic ether groups on the tetra-substituted benzene ring, shown in blue in Figure 4a, give rise to three coplanar transition moment vectors separated by an angle θ. The molecule is represented schematically in Figure 4b, in which the rigid backbone is represented by a red line and the transition moment vectors by three blue lines. This is the same schematic figure used in Figures 3a and 3b. Therefore, it is clear that two factors will influence the dichroic ratio of the aromatic ether stretching peak: the overall extent of orientation of the molecules, and the angle θ between the transition moment vectors.

A third factor which will also influence the dichroic ratio of the aromatic ether stretching peak is most easily understood by observing a three-dimensional computer model of the molecule produced with CambridgeSoft

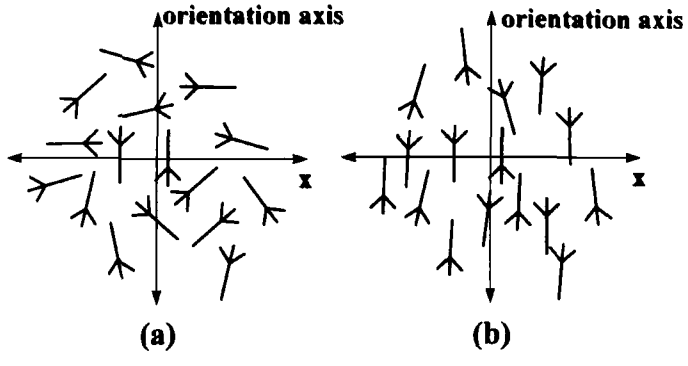

FIGURE 3 Molecules featuring three coplanar transition moment vectors separated by an angle θ. **a** Random orientation. **b**. Less-than perfect uniaxial orientation.

Chem3D molecular modeling software. Focusing on the rigid backbone portion of the molecule in Figure 5, it is clear that the tetra-substituted benzene ring is not coplanar with the backbone para-substituted benzene rings. The conformation of the tetra-substituted benzene ring relative to the backbone para-substituted benzene rings will also influence the dichroic ratio of the aromatic ether stretching peak.

Three factors determine the dichroic ratio of the aromatic ether stretching peak: the overall extent of orientation of the molecules, the conformation of the tetra-substituted benzene ring relative to the backbone para-substituted benzene rings, and the angle θ between the aromatic ether bonds. Thus,

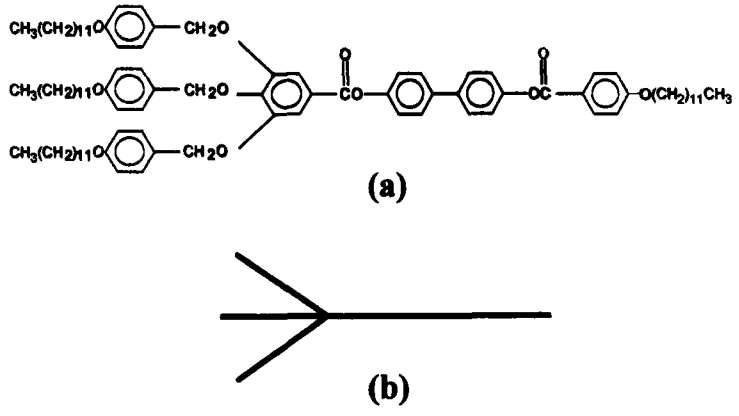

FIGURE 4 a. Liquid crystalline molecule being studied. b. Schematic representation of molecule.

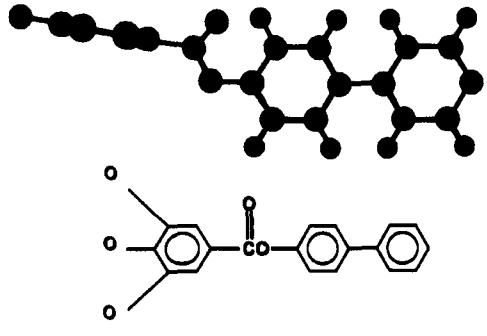

FIGURE 5 Three-dimensional model of backbone portion of molecule and two-dimensional representation of same region of molecule.

once the overall extent of orientaion of the molecules and the conformation of the benzene rings relative to each other are measured, these values can be combined with the dichroic ratio of the aromatic ether stretching peak to measure the angle between the aromatic ether bonds.

Although vibrational coupling between the aromatic ether stretching vibration and benzene "ring breathing" vibration [4, 5], can rotate the aromatic ether stretching transition moment vectors so that they do not lie directly along the C_{aryl}—O bonds, the angle between the transition moment vectors will always equal the angle between the chemical bonds; thus the angle between the bonds can be measured with infrared spectroscopy.

The three variables above can be obtained by measuring and comparing the dichroic ratio of various peaks in the infrared spectrum of the liquid crystal. However, no analysis can be performed if the sample is randomly oriented and the dichroic ratios of all peaks are equal to 1. Therefore, samples containing some amount of moelcular orientation must be prepared. This was done using NaCl plates coated with a thin, transparent layer of uniaxially rubbed polyimide; when the material is in a liquid crystalline mesophase, the molecules will align to some extent along the polyimide rubbing direction. This is evidenced by the two infrared spectra shown in Figure 6, which were procured with the material in the smectic C mesophase and the electric vector of the infrared beam polarized parallel and perpendicular to the polyimide rubbing direction, respectively. The

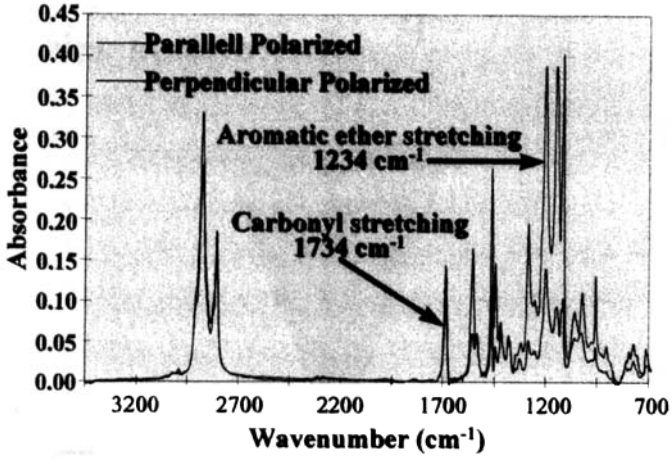

FIGURE 6 Infrared spectra of the material in the smectic C mesophase.

extensive dichroism confirms that the molecules are preferentially uniaxially oriented. Two peaks which will be relevant to the analysis, the carbonyl stretching peak at 1734 cm^{-1} and the aromatic ether stretching peak at 1234 cm^{-1}, are highlighted.

The rubbed polyimide plates provide less-than-perfect uniaxial orientation of the molecules. The first step which must be taken towards measuring the angle between the aromatic ether bonds is to determine precisely the extent to which the molecules are oriented at each temperature of interest. This was done by first assuming the rigid backbones of all the molecules are arranged in a cone of semiangle β around the orientation axis [6–8] as shown in Figure 7. The value of the cone semiangle β is indicative of the extent of orientation of the molecules; if $\beta = 0°$, the molecules are perfectly oriented along the orientation axis and the dichroic ratio, R, of a peak arising from a transition moment vector aligned along the backbone is infinite; if $\beta = 54.73°$, $R = 1$; and if $\beta = 90°$, $R = 0$. Because β is indicative of the extent of uniaxial orientation, measuring β at each temperature of interest is the first step which must be taken towards measuring the angle between the aromatic ether bonds. Clearly β is intrinsically linked with the dichroic ratio, therefore β can be calculated from the dichroic ratio of some peak in the infrared spectrum of the liquid crystal.

The molecule structure dictates which infrared absorbance peak can be analyzed to solve for β. Two carbonyl groups lie close to the rigid back-

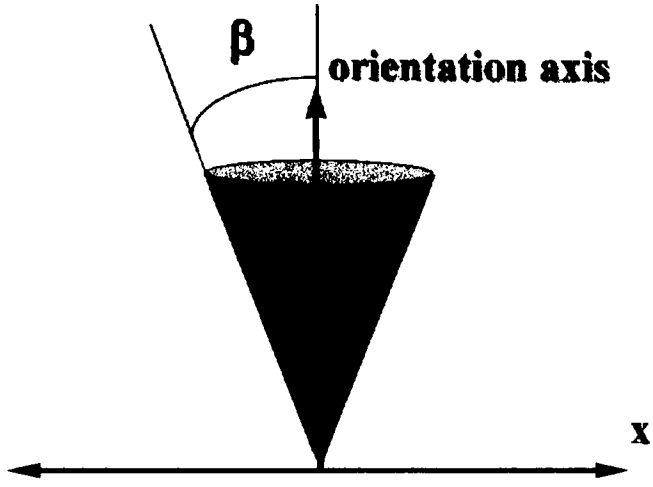

FIGURE 7 Backbones arranged in a cone of semiangle β about the orientation axis.

bone, which is defined by the adjacent para-substituted benzene rings as shown in Figure 8a. It is well noted in the literature [9] that when an ester group is attached to a benzene ring, as in this molecule, the transition moment vector for the carbonyl stretching vibration makes an angle of 60° to the backbone, as shown in Figure 8b. Knowing this, an equation relating the dichroic ratio of the carbonyl stretching infrared absorbance peak to the value of the cone semiangle β can easily be derived [10] and is shown below:

$$\beta = \cos^{-1}\sqrt{\frac{R\cos^2\alpha - \sin^2\alpha + 1/2\,R\sin^2\alpha}{2\cos^2\alpha - \sin^2\alpha + R\cos^2\alpha - 1/2\,R\sin^2\alpha}} \tag{1}$$

R is the dichroic ratio of the carbonyl stretching peak, β the cone semiangle, and α the angle the carbonyl stretching transition moment vector makes with the backbone; in this case $\alpha = 60°$. The dichroic ratio of the carbonyl stretching peak can be measured at each temperature of interest and then inserted into the equation above to measure β at each temperature. This is the first step which must be taken towards measuring the angle between the aromatic ether bonds.

The second step which must be taken towards measuring the angle between the aromatic ether bonds is to measure the conformation of the tetra-substituted benzene ring relative to the backbone para-substituted

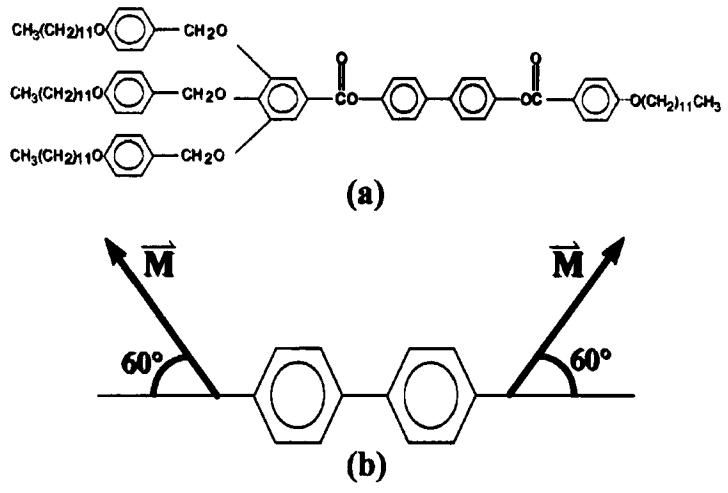

FIGURE 8 a. Structure of molecule, with carbonyl groups and backbone highlighted. b. Position of carbonyl stretching transition moment vector relative to backbone.

benzene rings. The complexity of the infrared spectrum of this material and vibrational coupling effects prevent the use of infrared spectra to measure the conformation of the benzene rings, however, a computer model of the molecule was used to obtain this information.

The third and final step which must be taken towards measuring the angle between the aromatic ether bonds is to measure the dichroic ratio of the aromatic ether stretching peak. Following the same type of derivation as above, an equation can be derived relating the dichroic ratio of this peak to the angle between the aromatic ether bonds, taking into account the overall orientation of the molecules and the conformation of the tetra-substituted benzene ring relative to the backbone para-substituted benzene rings [11]. This equation is shown below:

$$R = \frac{\begin{array}{c}[(M+2M\cos\theta)^2\cos^2\phi_1 + 2(M+2M\cos\theta)(2M\sin\theta)\cos\phi_1\sin\phi_2\sin\phi_1 \\ +(2M\sin\theta)^2\sin^2\phi_2\sin^2\phi_1]\cos^2\beta \\ +\frac{1}{2}[M+2M\cos\theta)^2\sin^2\phi_1 + 2(M+2M\cos\theta)(2M\sin\theta)\sin\phi_1\sin\phi_2\cos\phi_1 \\ +(2M\sin\theta)^2\sin^2\phi_2\cos^2\phi_1]\sin^2\beta + \frac{1}{2}(2M\sin\theta)^2\cos^2\phi_2\sin^2\beta\end{array}}{\begin{array}{c}\frac{1}{2}[(M+2M\cos\theta)^2\cos^2\phi_1 + 2(M+2M\cos\theta)(2M\sin\theta)\cos\phi_1\sin\phi_2\sin\phi_1 \\ +(2M\sin\theta)^2\sin^2\phi_2\sin^2\phi_1]\sin^2\beta + \frac{1}{4}(M+2M\cos\theta)^2\sin^2\phi_1 \\ +2(M+2M\cos\theta)(2M\sin\theta)\sin\phi_1\sin\phi_2\cos\phi_1 \\ +(2M\sin\theta)^2\sin^2\phi_2\cos^2\phi_1]\cos^2\beta + \frac{1}{4}[(M+2M\cos\theta)^2\sin^2\phi_1 \\ +2(M+2M\cos\theta)(2M\sin\theta)\sin\phi_1\sin\phi_2\cos\phi_1 \\ +(2M\sin\theta)^2\sin^2\phi_2\cos^2\phi_1] + \frac{1}{4}(2M\sin\theta)^2\cos^2\phi_2\cos^2\beta \\ +\frac{1}{4}(2M\sin\theta)^2\cos^2\phi_2\end{array}} \quad (2)$$

R is the dichroic ratio of the aromatic ether stretching peak, β the cone semiangle, and θ the angle between the aromatic ether bonds. The rotational and torsional angles used to measure the conformation of the tetra-substituted benzene relative to the backbone parasubstituted benzenes are labeled as ϕ_1 and ϕ_2, respectively. As will be discussed below, in this case $\phi_1 = 11.3°$ and $\phi_2 = 70.5°$. Note that M, the magnitude of the transition moment vector for the aromatic ether stretching vibration, cancels out of this equation.

EXPERIMENTAL

Synthesis of the liquid crystal is documented by Shenouda *et al.* [12]. Infrared spectroscopic cell preparation is shown schematically in Figure 9. An NaCl plate coated with a rubbed polyimide layer was sprayed with 5 μm glass spacers. Another NaCl plate, also with a rubbed polyimide coating, was then placed on top of the first plate so that their rubbed polyimide layers were facing each other; the glass spacers ensured a 5 μm space between the plates. These plates were epoxied together to make the cell, which was then placed in an Omega CN5000 digital heating stage. An Omega Ch/Al thermocouple was epoxied directly to the side of the cell and attached to an Omega HH21 digital thermometer to enable accurate sample temperature measurement during spectra acquisition. This entire apparatus, along with a Specac quartz polarizer, was then placed in a Bio-Rad FTS-60 Fourier transform infrared spectrometer to procure spectral backgrounds. Two backgrounds were procured, each with 64 scans at $4\,cm^{-1}$ resolution. The first background was procured with the electric vector of the incident infrared beam polarized parallel to the polyimide rubbing direction; the second background was procured with the electric vector of the incident infrared beam polarized perpendicular to the polyimide rubbing direction. The first background was used when acquiring spectra with the electric vector of the incident infrared beam polarized parallel to the polyimide rubbing direction, and the second background was used when acquiring spectra with the electric vector of the incident infrared beam polarized perpendicular to the polyimide rubbing direction. After acquiring the backgrounds, the apparatus containing the cell was heated on a hot stage and the 5 μm space between the coated plates was filled with the liquid crystal by capillary action.

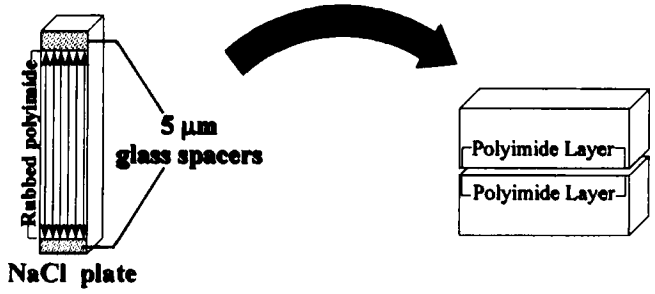

FIGURE 9 Preparation of infrared spectroscopic cell.

Based on the schematic phase diagram[13, 14] in Figure 10, experiments were performed by heating the liquid crystal to the isotropic phase and then acquiring spectra while cooling through the liquid crystalline mesophases. The phase transition temperatures were confirmed using DSC at a cooling rate of 5°C/min. The DSC trace in Figure 11 clearly shows the isotropic/ne-

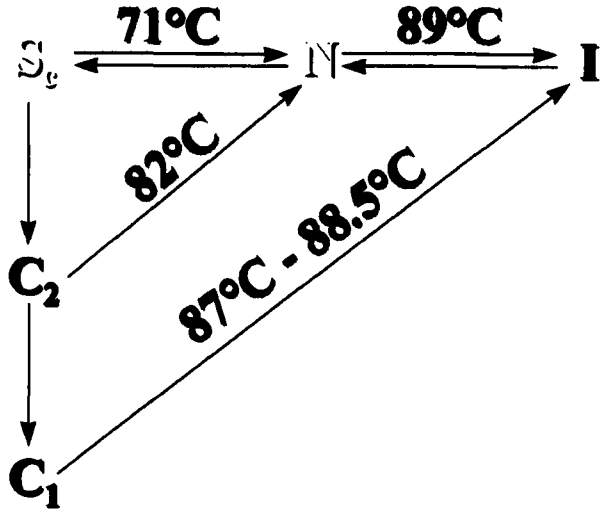

FIGURE 10 Schematic phase diagram of 4-[3′,4′,5′-Tri(*p*-*n*-dodecyloxybenzoyloxy)benzoyloxy]4″-*p*-*n*-dodecyloxybenzoyloxy-biphenyl.

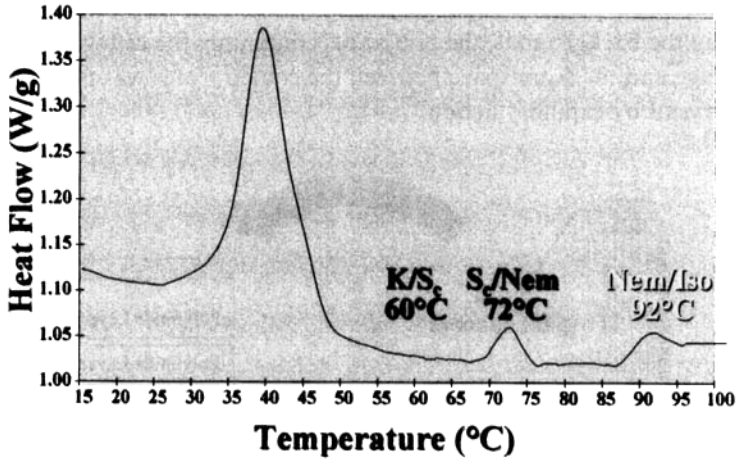

FIGURE 11 DSC trace procured at a cooling rate of 5°C/min.

matic transition at 92°C and the nematic/smectic C transition at 72°C. The smectic C crystallization temperature is listed as 60°C; this is supported by spectroscopic evidence. Based on the DSC results, spectra procured between 61°C and 91°C were analyzed.

The sample was placed in the Bio-Rad FTS-60 and heated to 100°C using the Omega CN5000 digital heating stage. One parallel—and one perpendicular-polarized spectra were taken at this temperature; the lack of dichroism ensured that the material was in the isotropic phase. The sample was then cooled to 91°C and two polarized spectra were again taken; the extensive dichroism indicated that the material had undergone a phase transition to the nematic phase. The sample was then cooled by 1°C and two polarized spectra were again procured; this was repeated until spectra had been procured at 27 different temperatures between 91°C and 61°C.

The dichroic ratio of the carbonyl stretching peak was measured by applying a first-order baseline adjustment to the region of the spectrum between 1790 cm^{-1} and 1690 cm^{-1} and then fitting one Gaussian peak to the carbonyl stretching peak using the PEAKFIT curve-fitting program. The area underneath the carbonyl stretching peak, which equals the infrared absorbance arising from the carbonyl stretching vibration, was reported by the curve-fitting program. Also reported for each peak fit was the error in the peak area; this error was incorporated into the analysis of each peak using typical error propagation methods.

The dichroic ratio of the aromatic ether stretching peak was measured by first performing a second-order baseline adjustment to the region of the spectrum between 1553 cm^{-1} and 897 cm^{-1}. Using PEAKFIT, the region between 1356 cm^{-1} and 1132 cm^{-1} was then fit with the corresponding peaks as shown in Figure 12. The errors reported by PEAKFIT for each peak were small, indicating an accurate fit. The peak arising from aromatic ether stretching of ether groups located on para-substituted benzenes occurs at 1252 cm^{-1}, while the peak arising from the same vibration of the ether groups on the tetra-substituted benzene occurs at 1234 cm^{-1}; both of these are in very good agreement with the literature values [15]. The peak at 1234 cm^{-1} was used to measure the angle between the aromatic ether bonds on the tetra-substituted benzene ring.

The dichroic ratio of the aromatic out-of-plane CH wagging peak arising from the tetra-substituted and backbone para-substituted benzene rings, respectively, was measured by first applying a first order baseline adjustment to the region of the spectrum between 900 cm^{-1} and 775 cm^{-1}. PEAKFIT was used to procure the fit shown in Figure 13, again with low errors. The peak arising from the tetra-substituted benzene ring is located at

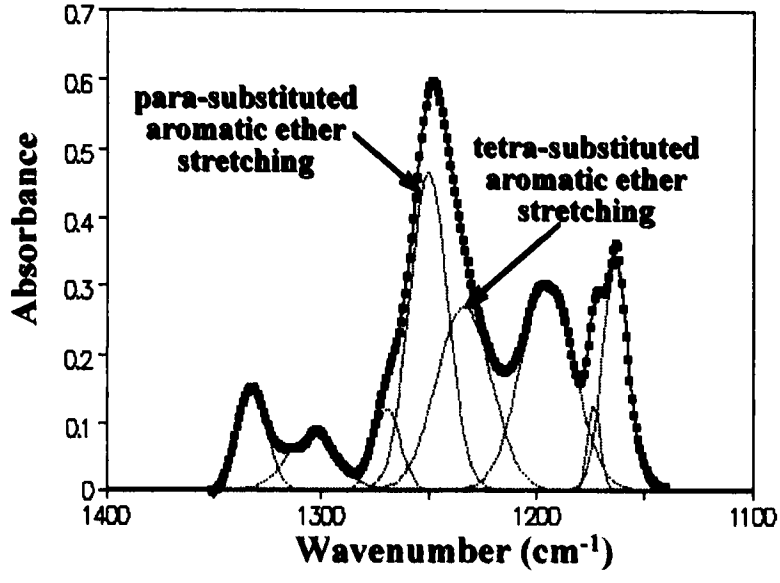

FIGURE 12 Deconvolution of aromatic ether stretching region of infrared spectrum.

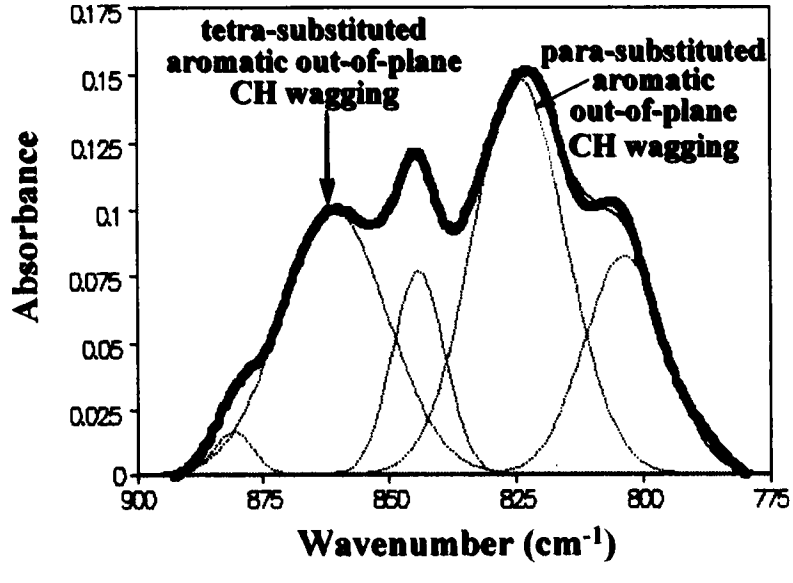

FIGURE 13 Deconvolution of aromatic out-of-plane wagging region of infrared spectrum.

865 cm^{-1}, and the peak arising from the backbone para-substituted benzenes is located at 825 cm^{-1} [16 – 18].

RESULTS

The dichroic ratio of the carbonyl stretching peak measured between 61°C and 91°C is shown in Figure 14. Because the transition moment vector of the carbonyl stretching vibration makes a rather large angle (60°) with backbone of the molecule, the dichroic ratio for this peak is less than 1, and it decreases as molecular orientation increases. The dichroic ratio decreases as the material is cooled through the nematic mesophase, indicating the molecules are following the expected trend of becoming more oriented with decreasing temperature. There is a shift in the dichroic ratio at the phase transition as the molecules reorient themselves to pack into their new mesophase, then the dichroic ratio is constant throughout the smectic C mesophase. Each data point was used to calculate a value for β at that particular temperature; the β values are shown in Figure 15.

CambridgeSoft Chem3D molecular modeling software was used to measure the conformation of the tetra-substituted benzene ring relative to

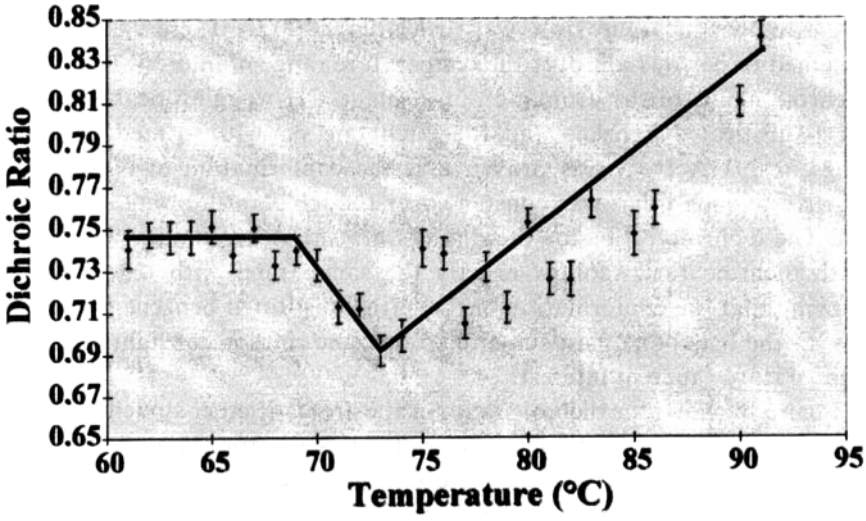

FIGURE 14 Dichoric ratio of carbonyl stretching peak versus temperature.

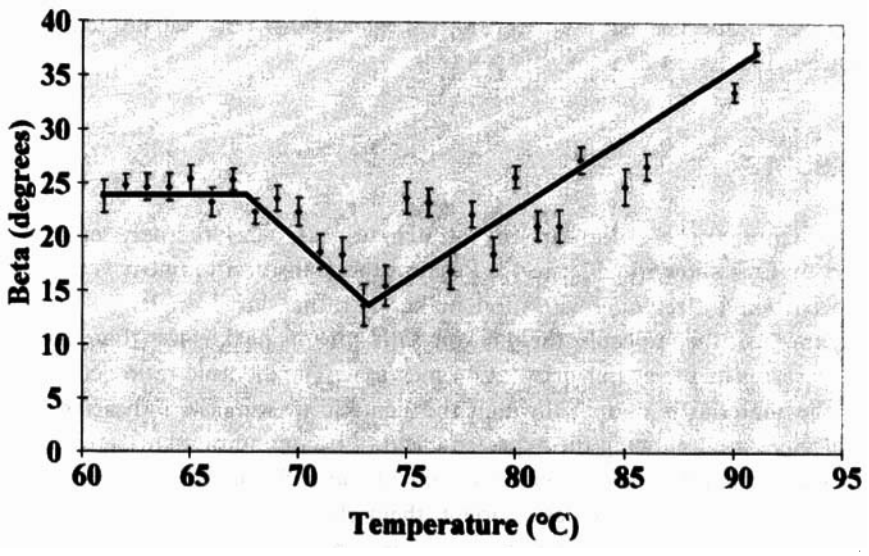

FIGURE 15 Cone semiangle β versus temperature.

the backbone parasubstituted benzene rings. Two angles were used to define the conformation of the rings relative to each other. The rotational angle, shown in Figure 16, was measured as 11.3°. The torsional angle, shown in Figure 16b, was measured as 70.5°. These values were assumed to be constant over the temperature range of interest. Using the dichroic ratios of the aromatic out-of-plane CH wagging peaks for the tetra-substituted benzene and the backbone para-substituted benzene rings, respectively, it was proven that the conformation of these rings relative to each other was constant over the temperature range of interest. The dichroic ratios for these peaks are shown in Figure 17. Clearly both dichroic ratios follow exactly the same trend with temperature, proving that the conformation of the tetra-substituted benzene ring relative to the backbone para-substituted benzene rings is constant over the temperature range of interest.

Figure 18 shows the dichroic ratio for the aromatic ether stretching peak. Because the transition moment vectors for this vibration are aligned generally along the long axis of the molecule, the dichroic ratio is greater than 1. There is a clear discontinuity in the dichroic ratio at 71°C, which is the phase transition temperature between the nematic and smectic C mesophases.

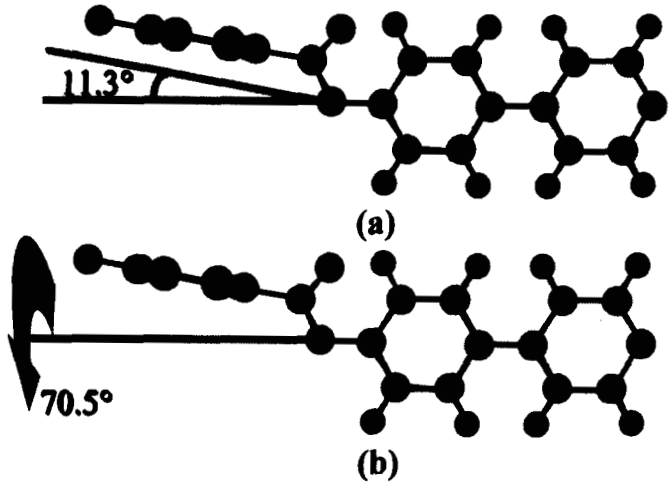

FIGURE 16 Conformation of tetra-substituted benzene ring relative to backbone para-substituted benzene rings. a Rotational angle. b. Torsional angle.

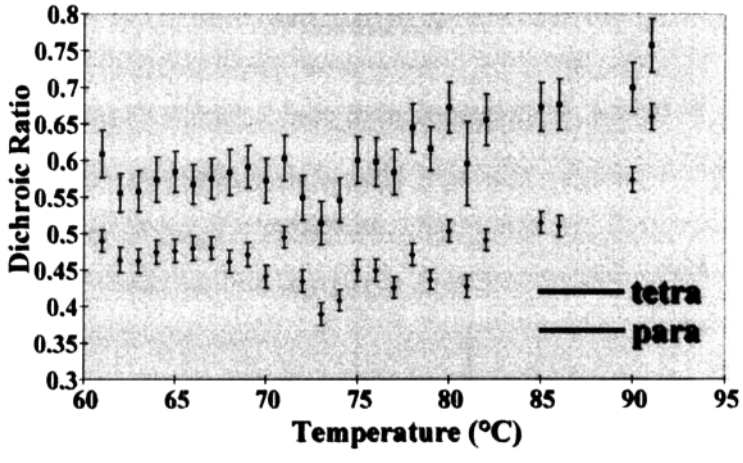

FIGURE 17 Dichroic ratios for aromatic out-of-plane wagging peaks from tetra-substituted and backbone para-substituted benzenes.

Using Equation 2, which includes the values for the dichroic ratio of the aromatic ether stretching peak from Figure 18, the β values from Figure 15, and the angles between the tetra-substituted and backbone para-substituted benzene rings as measured from the Chem3D software, the angle between

the aromatic ether bonds was calculated at each temperature of interest. The values for the angle between the aromatic ether bonds are shown in Figure 19. There is a clear decrease in the angle between the bonds at the transition between the nematic and smectic C mesophases.

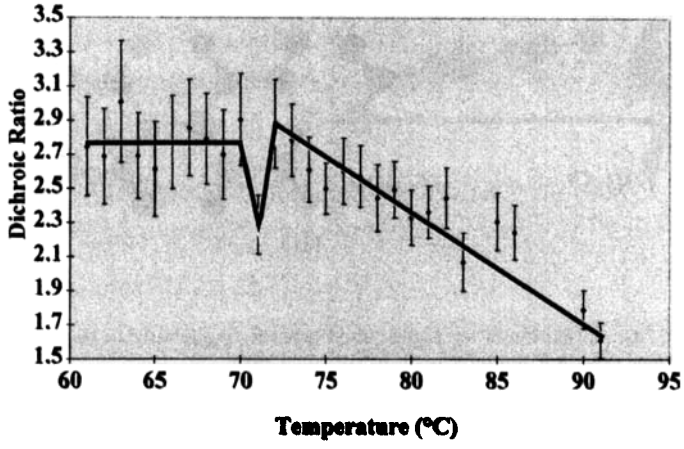

FIGURE 18 Dichoric ratio of 1234 cm^{-1} aromatic ether stretching peak versus temepera-ture.

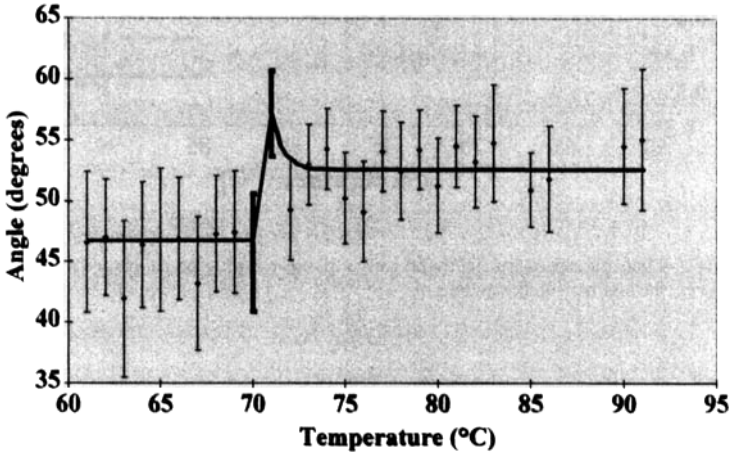

FIGURE 19 Angle between aromatic ether bonds versus temperature.

DISCUSSION

The data provides evidence that the abrupt decrease in the measured angle between the aromatic ether bonds at the phase transition is attributable to a decrease in the angle between the bonds, and not an overall reorientation of the molecules or a change in the conformation of the tetra-substituted benzene ring relative to the backbone para-substituted benzene rings at the phase transition. Because the value of β, which is indicative of the extent of overall orientation of the molecules, is included in Equation 2, then any change in the overall orinetation of the molecules at the phase transition is taken into account when calculating the angle between the aromatic ether bonds. Also, it was proven that the conformation of the tetra-substituted benzene ring relative to the backbone para-substituted benzene rings was constant over the temperature range of interest. Thus the decrease in the measured angle between the aromatic ether bonds is attributable only to a decrease in the angle between the bonds.

The measured decrease in the angle between the aromatic ether bonds also cannot be attributed to any scattering of the infrared beam at the phase transition. An increase in scattering of the beam because of the phase transition would result in an increase in the noise of the spectrum procured at the phase transition. This was not observed; the signal-to-noise ratio was constant for all spectra. Thus, the measured decrease in the angle between the aromatic ether bonds is not caused by any scattering effects.

The decrease in the angle between the aromatic ether bonds precede the phase transition from the nematic to the smectic C mesophase. At the phase transition from the nematic to the smectic C mesophase, the material passes from a less-ordered to a more-ordered phase. Packing into the more highly ordered phase is facilitated by the decrease in the angle between the aromatic ether bonds, which places the molecule in a more compact conformation.

The data provides evidence that there is a decrease in the angle between the aromatic ether bonds, regardless of the validity of the two assumptions made in the analysis. First, the angle between the aromatic ether bonds was calculated at each temperature assuming an absence of coupling between the aromatic ether stretching vibration and any benzene ring vibrations. If this assumption is incorrect, reanalysis of the data including any effect of coupling will only shift the data in Figure 19 on the y axis; it will not change the trend of the data with temperature. Also, the conformation of the tetra-substituted benzene ring relative to the backbone para-substituted rings was measured using molecular modeling software. If the actual confor-

mation differs from that measured with the software, again the only effect on the data in Figure 19 would be a shift on the y axis and not a change in the trend with temperature. Thus, the trend of the data with temperature is real. Also, based on the structure of benzene, it would be expected that the angle between the aromatic ether bonds be approximately 60°; the measured data is roughly between 45° and 60°. The proximity of the measured values to the expected value indicates that the assumptions made do not differ greatly, if at all, from the actual circumstance.

CONCLUSIONS

The angle between the aromatic ether bonds located on the tetra-substituted benzene ring in 4-[3′,4′,5′-Tri(*p-n*-dodecyloxybenzoyloxy)benzoyloxy]4″-*p-n*-dode cyloxybenzoyloxy-biphenyl was measured in both the nematic and smectic C mesophases. An abrupt decrease in the angle between the aromatic ether bonds occured at the phase transition from the nematic to the smectic C mesophase. The transition from the nematic to the smectic C mesophase results in a more compact conformation of the molecule.

Acknowledgement

This work was supported by ALCOM grant DMR89-20147.

References

[1] P. G. de Gennes and J. Prost, *The Physics of Liquid Crystals*, 2nd Edition, (Clarendon Press, New York, 1993), p. 3.
[2] P. Collings, *Liquid Crystals: Nature's Delicate Phase of Matter*. Princeton Science Library, (Princeton, NJ, 1990), p. 12.
[3] J. L. Koenig, *Spectroscopy of Polymers*, (American Chemical Society, Washington, D.C., 1992), p. 26.
[4] H. L. Hergert, "Infrared Spectra", In *Lignins: Occurence, Formation, Structure, and Reactions*, K. V. Sarkanen and C. H. Ludwig, Eds., (Wiley-Interscience, New York, 1971), p. 272.
[5] K. V. Sarkanen, Chang, Hou-Min and G.G. Allan, *Tappi*, **50**(11), 572 (1967).
[6] R. D. B. Fraser, *The Journal of Chemical Physics*, **21**(9), 1511 (1953).
[7] J. L. Koenig, *Spectroscopy of Polymers*, (American Chemical Society, Washington , D.C., 1992), p. 27.
[8] H. W. Siesler, *Adv. Polymer Science*, **65**, 2 (1984).
[9] K. H. Kim, K. Ishikawa, H. Takezoe and A. Fukuda, *Physical Review, E*, **51**(3), 2166 (1995).
[10] R. D. B. Fraser, *The Journal of Chemical Physics*, **21**(9), 1511 (1953).
[11] M. S. Thesis and C. S. DiGiacomo, Case Western Reserve University.
[12] I. G. Shenounda, Y. Shi and M. E. Neubert, *Mol. Cryst. Liq. Cryst.*, **257**, 209 (1994).

[13] J. Malthete, L. Liebert, A. Levelut and Y. Galerne, *C. R. Acad. Sc. Paris, Series II*, **303**(12), 1073 (1986).
[14] J. Malthete and P. Davidson, *Bull Soc Chim Fr*, **131**, 812 (1994).
[15] W. Collier, T. Schultz and V. Kalasinsky, *Hoklzforschung*, **46**(6), 523.
[16] G. Varsanyi, *Vibrational Spectra of Benzene Derviaties*, (Academic Press, New York, 1969), p. 152.
[17] G. Varsanyi, *Assignments for Vibrational Spectra of Seven Hundred Benzene Derivatives*, (Wiley, New York, 1974), p. 382.
[18] Sadtler Standard Spectrum ≠8449, 3,4,5-trimethoxy benzoic acid, Sadtler Research Laboratories, Philadelphia, Pennsylvania.